

Supporting Information

Control of electronic symmetry and rectification through energy level variations in bilayer molecular junctions

*Akhtar Bayat, Jean-Christophe Lacroix, and Richard L. McCreery**

Akhtar Bayat, R. L. McCreery
University of Alberta, 11421 Saskatchewan Dr. Edmonton, AB T6G 2M9, Canada
E-mail: McCreery@ualberta.ca

Jean-Christophe Lacroix
University of Paris, Diderot

R. L. McCreery
National Institute for Nanotechnology, 11421 Saskatchewan Dr. Edmonton, AB T6G 2M9, Canada

* corresponding author

1. Junction fabrication and bilayer deposition
2. Molecular layer thickness determination
3. Single and bilayer UV-Vis absorption spectra
4. NDI and NDI/BTB XPS spectra
5. *JV* curves for NDI/BTB in air and vacuum
6. Reproducibility of *JV* curves
7. Effect of NDI thickness on NDI/BTB *JV* curves

1. Junction fabrication:

Pyrolyzed photoresist film (PPF) stripes with the width of 0.5 mm were made on thermally oxidized silicon chips as described previously^{1,2}. Molecular bilayers were made by successive electro-reduction of two different diazonium salts on the PPF working electrode in a three-electrode cell with a platinum wire as counter electrode and Ag/Ag⁺(Fc/Fc⁺ located at +0.1V) as reference electrode.

In a typical procedure for deposition of the first layer, a solution of 0.5 mM NDI diazonium salt in 0.1 M tetrabutylammonium tetrafluoroborate (TBABF₄) in anhydrous acetonitrile (ACN) was bubbled with argon gas for 10 min. The Si/SiO_x chip with PPF lines was put in solution as working electrode and cyclic voltammetry was performed by sweeping the voltage from 0.4 V to -0.6 V at 0.05 V/s for 10 cycles to give ~10.7 nm layer of NDI on PPF stripes. The conditions for modification of PPF with AQ, FL and BTB as the first layer of the bilayer are presented in Table S1. After modification of PPF stripes with the first layer, the chip was rinsed with ACN and dried with a stream of nitrogen gas.

To form the second layer of the bilayer, cyclic voltammetry was performed in a solution of the diazonium salt of the second layer or the diazonium ions were generated “in-situ”³⁻⁵. As an example for the in-situ method, 20 mL of 0.5 mM BTB solution of amine precursor (Figure S1) solution in 0.1 M TBABF₄ in ACN was bubbled for 10 min with argon gas and 60 μL of t-butyl nitrite was added to the solution to form a bright red solution. The PPF chip already modified with NDI as the first layer was put in the solution as working electrode and the voltage was swept from 0 to -1.2 V at 0.05 V/s for 10 cycles to form a ~10.3 nm BTB layer on top of the 10.7 nm NDI layer which amounts to a total thickness of NDI-BTB bilayer of 21 nm. The conditions for the deposition of BTB, AQ, NAB and FL layers as the second layer on top of various first layers are presented in Table S1.

During the deposition of AQ and FL as second layers or BTB on AQ, the solution was still being purged with argon gas to prevent the reduction of oxygen instead of the reagent. Argon bubbling during electrochemical modification was only necessary in these cases as the potential window is quite wide in the negative direction.

Large area cross-bar bilayer junctions with 250 by 500 μm dimensions (area= 0.00125 cm²) were completed by electron-beam deposition of e-carbon and gold as top contacts using an electron-beam evaporator (Kurt J. Lesker PVD75) at a typical chamber pressure of <5 ×10⁻⁶ Torr.

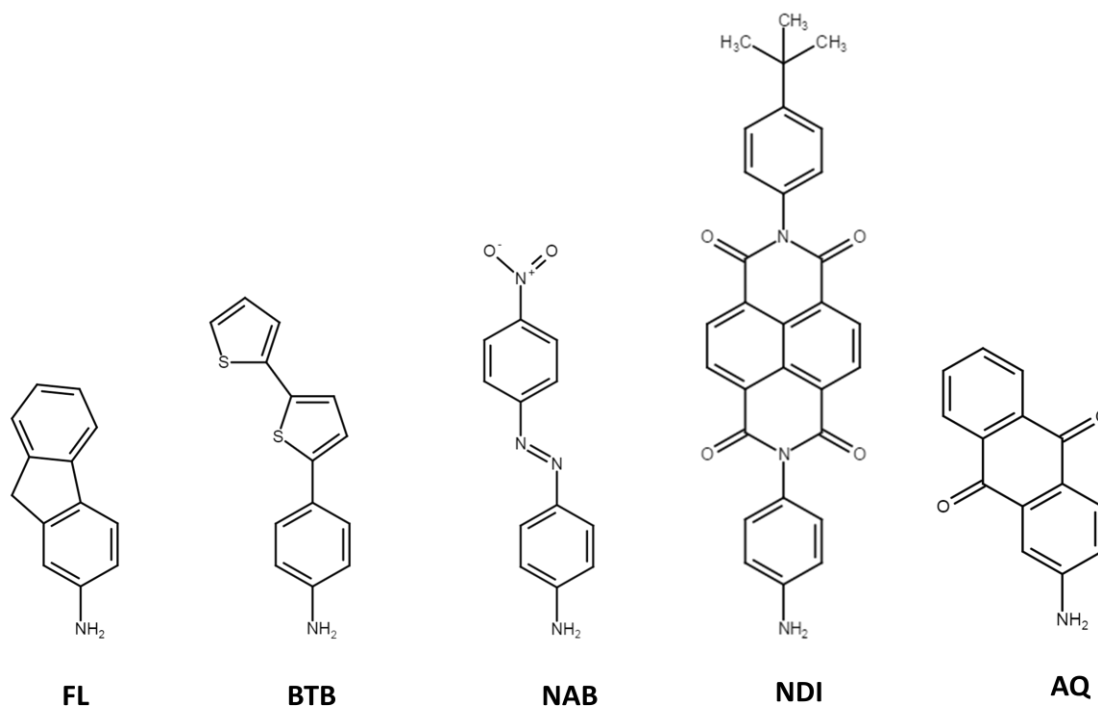


Figure S1: Structures of the amine precursors to diazonium reagents.

<i>layer</i>	<i>Solution in 0.1M TBABF₄ in ACN</i>	<i>CV conditions vs Ag/Ag⁺</i>	<i>thickness(nm)</i>
NDI	0.5 mM NDI DS	0.4 to -0.6 V at 0.05 V/s for 10 cycles	10.7 ± 0.7 nm
BTB on NDI	0.5 mM BTAB (20 mL) + 60μL t-butyl nitrite	0 to -1.2 V at 0.05 V/s for 10 cycles	10.3 ± 1 nm
AQ on NDI	1mM AQ DS	0.4 to -0.8 V at 0.05 V/s for 10 cycles	11.9 ± 0.7 nm
NAB on NDI	1mM NAB DS	0.4 to -0.8 V at 0.05 V/s for 10 cycles	11.4 ± 0.7 nm
FL on NDI	1mM FL DS	0.4 to -1.8 V at 0.05 V/s for 20 cycles (bubbling argon)	13 ± 0.8 nm
AQ	1mM AQ DS	0.4 to -0.65 V at 0.05 V/s for 10 cycles	8.4 ± 0.6 nm
FL on AQ	1mM FL DS	0.4 to -1.8 V at 0.05 V/s for 10 cycles (bubbling argon)	12.3 ± 0.8 nm
BTB on AQ	0.5 mM BTAB (20 mL) + 60μL t-butyl nitrite	0 to -1.8 V at 0.2 V/s for 20 cycles (bubbling argon)	11.6 ± 1 nm
FL	1mM FL DS	0.4 to -1.5 V at 0.05 V/s for 10 cycles	12 ± 1 nm
AQ on FL	1mM AQ DS	0.4 to -1.8 V at 0.05 V/s for 10 cycles (bubbling argon)	5.3 ± 0.9 nm
BTB	0.5 mM BTAB (20 mL) + 60μL t-butyl nitrite	0 to -0.8 V at 0.05 V/s for 10 cycles	11 ± 1 nm
AQ on BTB	1mM AQ DS	0 to -1.8 V at 0.2 V/s for 20 cycles	13 ± 4 nm

Table S1. Deposition conditions and layer thicknesses from AFM scratching². DS= the isolated fluoroborate salt of the corresponding diazonium ion.

2. Molecular layer thickness determination

All single and bilayer film thicknesses were verified by AFM “scratching”⁶, with the layer thickness determined statistically as shown in the example of NDI and NDI/BTB in figure S2 and discussed in detail in the Supporting Information of these references^{5,7}. The position of the “scratch” was adjacent to a functional junction, but away from the eC/Au top contact. The AFM setpoint “force” was determined empirically by increasing the force enough to remove the molecular layer but not damage or alter a bare PPF surface⁶.

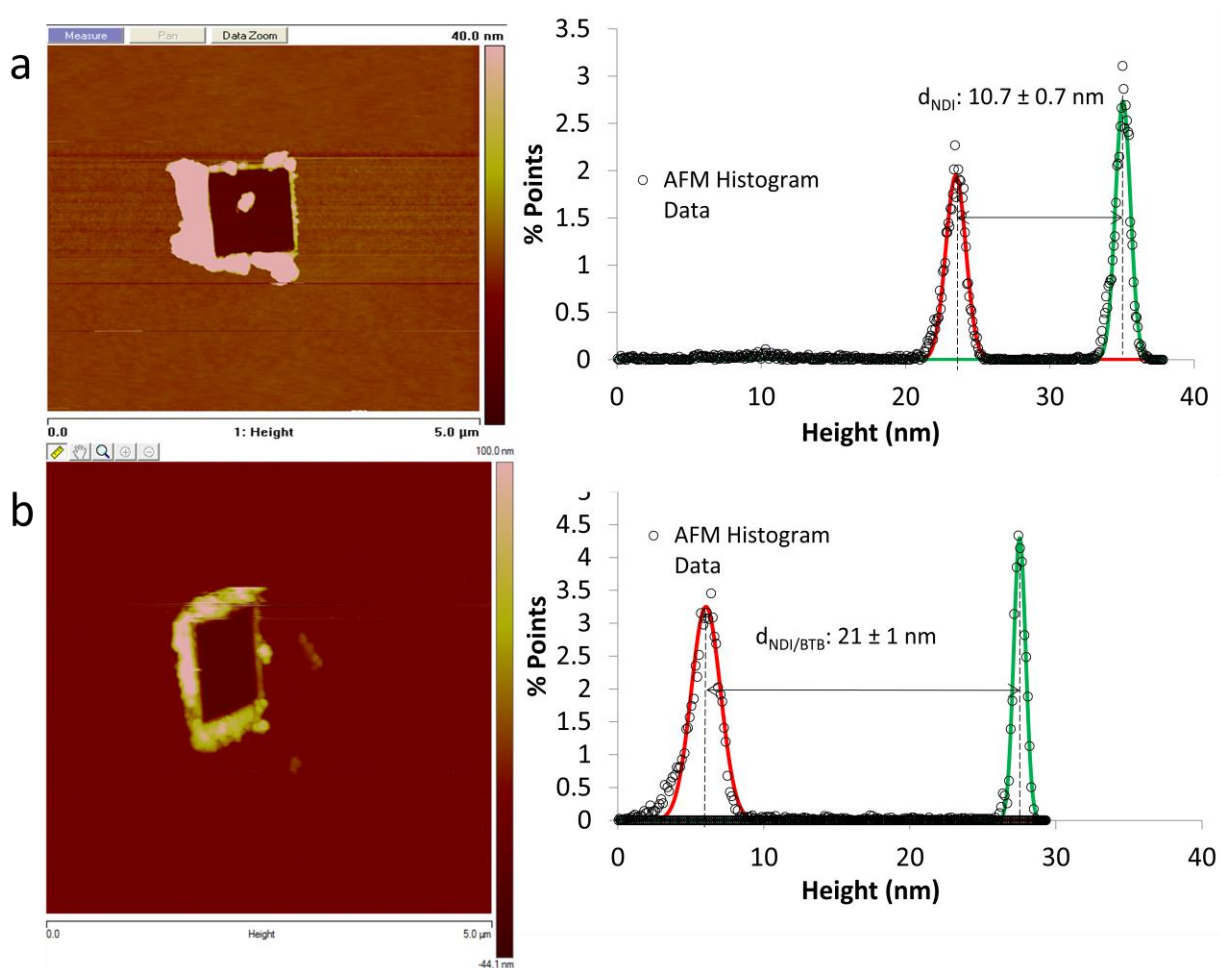


Figure S2: Examples of AFM trench images from scratching and depth histograms⁷ for (a) NDI layer and (b) NDI/BTB.

3. Single and bilayer UV-Vis absorption spectra

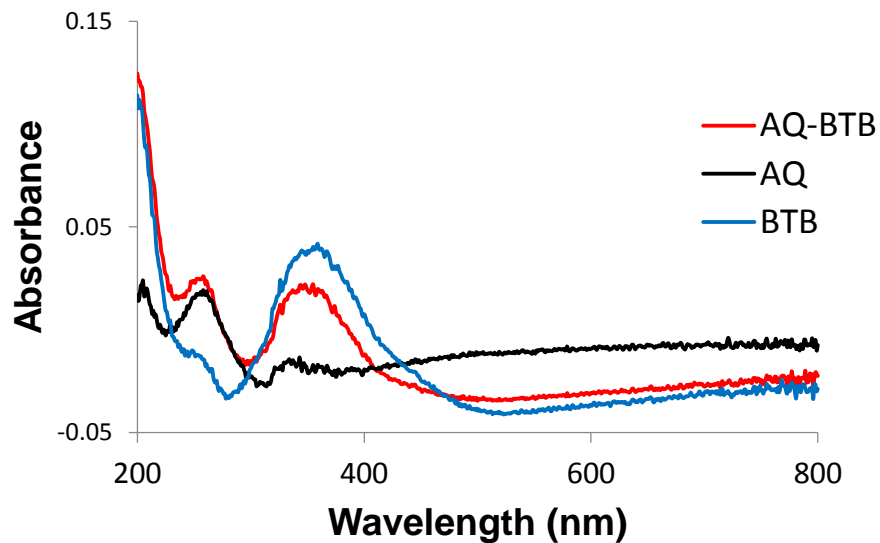


Figure S3: UV-Vis spectra of AQ, BTB and AQ/BTB bilayer on a quartz/Cr₃/Au₁₃/eC₇ substrate after subtraction of the spectrum of the unmodified substrate.

4. NDI and NDI/BTB XPS spectra

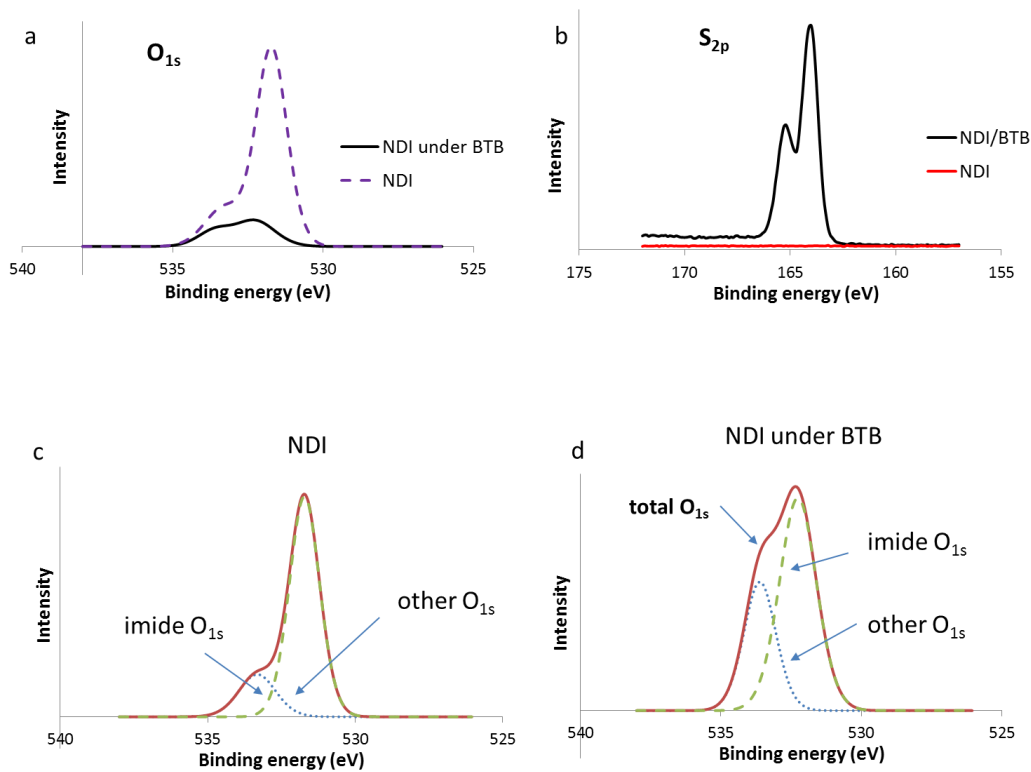


Figure S4: XPS spectra of NDI and NDI/BTB layers on PPF for **a.** O_{1s} region, **b.** S_{2p} region, **c.** O_{1s} components for NDI single layer and **d.** O_{1s} components for NDI/BTB bilayer.

	C	O (imide)	Other O	N	S
NDI	87.2%	7.3%	1.7%	3.7%	0%
NDI/BTB	85.8%	1.3%	0.66%	1.9%	9.3%

Table S2: Surface atom% ratios on modified PPF surfaces determined from XPS.

5. JV curves for NDI/BTB in air and vacuum

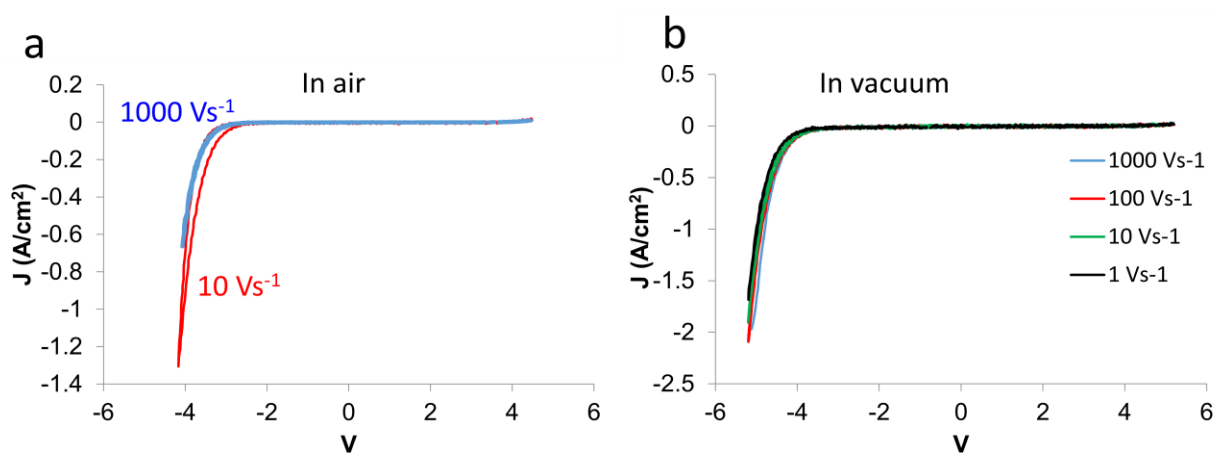


Figure S5: NDI/BTB bilayer J - V in **a.** Air and **b.** Vacuum at various scan rates. The hysteresis observed in air increased for slower scan rates.

6. Reproducibility of JV curves

As indicated in the main text, all JV curves presented are averages of at least four MJs of the same type, with the standard deviations of J and RR listed in Table 1 of the main text. Figure S6 shows several examples of JV curves with errors bars indicating \pm standard deviation.

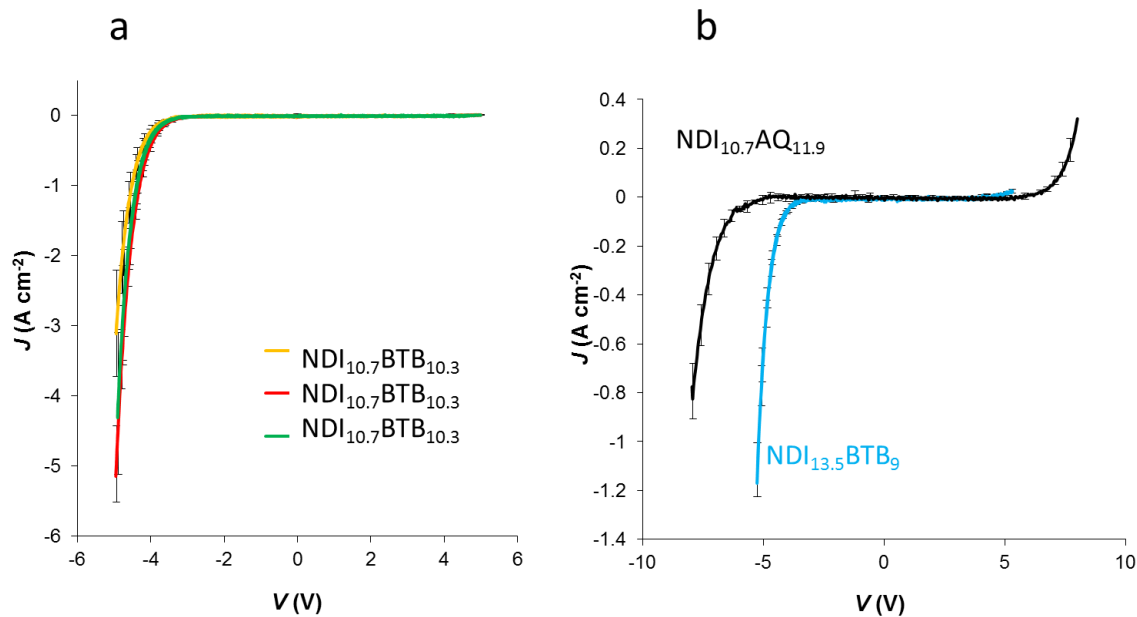


Figure S6. **a.** *JV* response for three different samples (chips) of NDI/BTB bilayer junctions, with error bars indicating \pm standard deviation for four junctions on each sample. **b.** *JV* response of the indicated bilayer junctions, with the same error bars.

7. Effect of NDI thickness on NDI/BTB *JV* curves

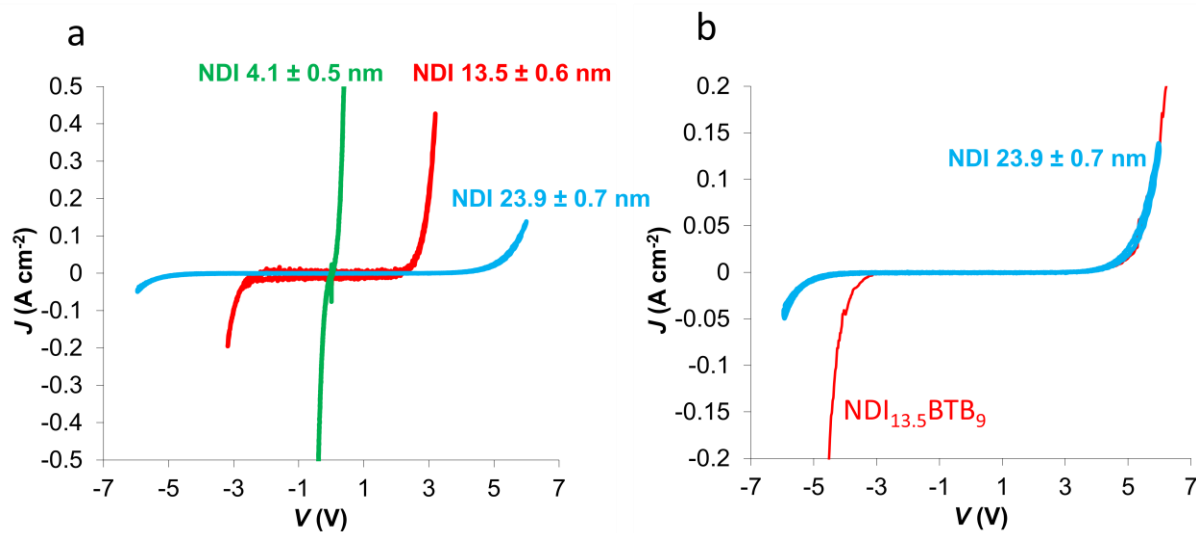


Figure S7: **a.** NDI layers with three different thicknesses, all showing symmetric *J-V* behavior. **b.** Thick NDI layer compared with NDI/BTB bilayer with similar thickness.

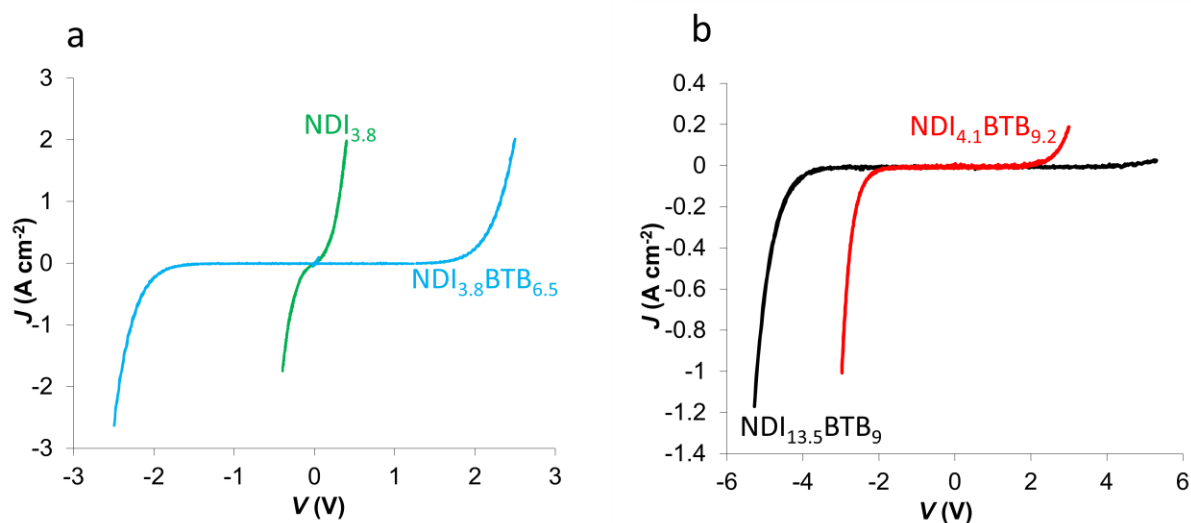


Figure S8: a. Thin NDI layer and thin NDI/BTB bilayer, showing symmetric J - V behavior.
b. The effect of the thickness of NDI on asymmetry of NDI/BTB bilayers.

References

- (1) Ru, J.; Szeto, B.; Bonifas, A.; McCreery, R. L.; *ACS Appl. Mater. Interfaces* **2010**, *2*, 3693-3701.
- (2) Anariba, F.; Steach, J.; McCreery, R.; *J. Phys. Chem. B* **2005**, *109*, 11163-11172.
- (3) Fluteau, T.; Bessis, C.; Barraud, C.; Della Rocca, M. L.; Martin, P.; Lacroix, J.-C.; Lafarge, P.; *J. Appl. Phys.* **2014**, *116*, 114509.
- (4) Fave, C.; Leroux, Y.; Trippe, G.; Randriamahazaka, H.; Noel, V.; Lacroix, J.-C.; *J. Am. Chem. Soc.* **2007**, *129*, 1890-1891.
- (5) Yan, H.; Bergren, A. J.; McCreery, R.; Della Rocca, M. L.; Martin, P.; Lafarge, P.; Lacroix, J. C.; *Proc. Natl. Acad. Sci.* **2013**, *110*, 5326-5330.
- (6) Anariba, F.; DuVall, S. H.; McCreery, R. L.; *Anal. Chem.* **2003**, *75*, 3837-3844.
- (7) Sayed, S. Y.; Fereiro, J. A.; Yan, H.; McCreery, R. L.; Bergren, A. J.; *Proc. Natl. Acad. Sci.* **2012**, *109*, 11498-11503.